

Magnetic trapping of Yb in the metastable 3P_2 state

Kanhaiya Pandey, K. D. Rathod, Sambit Bikas Pal, and Vasant Natarajan*

Department of Physics, Indian Institute of Science, Bangalore 560 012, India

(Received 23 November 2009; published 29 March 2010)

We report magnetic trapping of Yb in the excited 3P_2 state. This state, with a lifetime of 15 s, could play an important role in studies ranging from optical clocks and quantum computation to the search for a permanent electric dipole moment. Yb atoms are first cooled and trapped in the ground state in a 399-nm magneto-optic trap. The cold atoms are then pumped into the excited state by driving the $^1S_0 \rightarrow ^3P_1 \rightarrow ^3S_1$ transition. Atoms in the 3P_2 state are magnetically trapped in a spherical quadrupole field with an axial gradient of 110 G/cm. We trap up to 10^6 atoms with a lifetime of 1.5 s.

DOI: [10.1103/PhysRevA.81.033424](https://doi.org/10.1103/PhysRevA.81.033424)

PACS number(s): 37.10.Gh, 42.50.Wk, 32.10.Dk

I. INTRODUCTION

The metastable 3P_2 state of Yb, with a lifetime of 15 s [1], is important as a possible clock transition (similar to the nearby 3P_0 state [2]) and for quantum computation [3,4]. It is also potentially useful in experiments searching for a permanent electric dipole moment (EDM) because its closer proximity to states of opposite parity, compared to the ground state, enhances the EDM effect [5]. In addition, the paramagnetic nature of this state implies that the atomic EDM will be sensitive to the intrinsic EDM of the electron [6]. The ground state of Yb has total electronic angular momentum $j = 0$ and atoms cannot be magnetically trapped in this state. By contrast, atoms can be trapped in the metastable state because $j = 2$. The magnetically trapped atoms can be further cooled using evaporative cooling or used directly for measurements. Such atoms are already spin polarized, an important prerequisite for EDM measurements. Magnetic trapping allows the study of interatomic collisions [7,8], which could be important for clock applications or obtaining Bose-Einstein condensation (BEC) in the metastable state. BEC in the metastable state will differ from that of the spin-zero ground state [9–12], and magnetic trapping may provide a new route to observing BEC. The large Landé g factor of the 3P_2 state makes it attractive for the study of dipolar magnetic interactions. Dipolar interactions have been studied in optical traps [13,14] but can be expected to be different in magnetic traps.

In this work, we demonstrate magnetic trapping of ^{174}Yb in the 3P_2 state. The relevant low-lying energy levels of Yb are shown in Fig. 1. As in the case of alkaline-earth-metal atoms, Yb has two transitions that can be used for laser cooling before loading the magnetic trap—the strongly allowed $^1S_0 \rightarrow ^1P_1$ transition at 399 nm and the weak $^1S_0 \rightarrow ^3P_1$ intercombination line at 556 nm. Both lines have been used previously for laser cooling [15–18]. In this study, we use the strong 399-nm line. The atoms are first cooled and trapped in a magneto-optic trap (MOT). In contrast to recent experiments on trapping of Sr in the metastable state [19], where a significant fraction of atoms is automatically transferred into the metastable state during operation of the MOT, our experiment requires active pumping of the atoms into the metastable state by driving a

transition to the upper 3S_1 state through the intermediate 3P_1 state. Atoms from the 3S_1 state partially decay into the 3P_2 state. About 10^7 atoms are captured in the MOT, and more than 10% are transferred into the magnetic trap. The trap is formed by a spherical quadrupole magnetic field with an axial gradient of 110 G/cm. The trap has a lifetime of 1.5 s, limited primarily by the vacuum. We demonstrate both pulsed and continuous loading of the trap from the MOT.

II. EXPERIMENTAL DETAILS

The main experimental chamber is shown schematically in Fig. 2. The trapping is done in a pyrex chamber with seven intersecting viewports (octagonally placed) in the horizontal plane and two viewports in the vertical plane. All viewports are 30 mm in diameter. The vertical plane has a pair of anti-Helmholtz coils to produce the required quadrupole field. The glass chamber is connected to a stainless steel cross with a 40-l/s ion pump on one side and an all-metal valve on the other. This is connected to the Yb source through a small differential pumping tube. When the source is on, the pressure inside the main chamber is below 10^{-8} torr, while the source side is up to two orders of magnitude higher.

The source consists of metallic Yb in a quartz ampoule that is resistively heated to about 400°C. The source contains

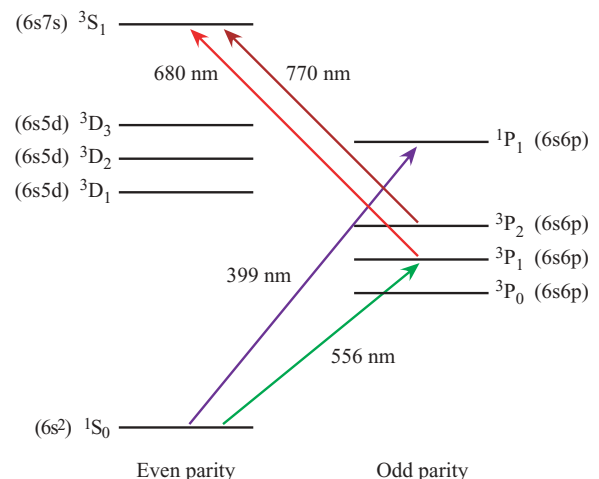


FIG. 1. (Color online) Low-lying energy levels of Yb showing the relevant transitions used in the experiment.

*vasant@physics.iisc.ernet.in; URL: www.physics.iisc.ernet.in/~vasant

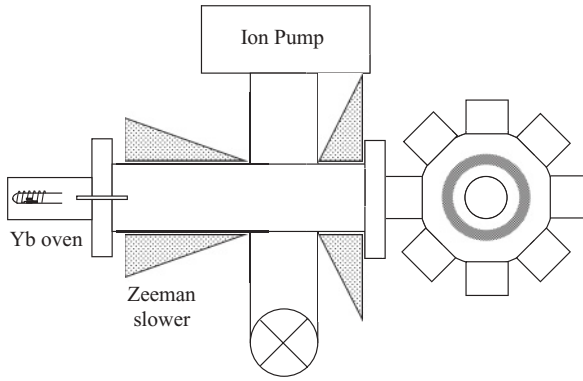


FIG. 2. Top view of the experimental vacuum chamber.

all isotopes in their natural abundances. The atoms emanate with a longitudinal rms velocity of 250 m/s. The velocity is slowed down to 20 m/s (the capture velocity of the MOT) using a spin-flip Zeeman slower [20], which consists first of a decreasing field part and then an increasing field region near the end. The total slowing distance is 45 cm, and the magnetic field varies from 210 G at the beginning to -235 G at the end. The slowing light is at 399 nm (same as the MOT beams) but is detuned by an additional -300 MHz.

A. Laser spectroscopy and locking

The energy-level diagram shows that the experiment requires the simultaneous operation of four lasers. The slower and MOT laser beams are at 399 nm. This is produced by using a ring Ti:sapphire laser (Coherent 899-21) operating at 798 nm and doubling its output in an external cavity doubler (Laser Analytical Systems LAS100). The output power of the Ti:sapphire is 1.4 W, and its frequency is stabilized on a reference cavity to give an rms linewidth of 1 MHz. The output of the doubler is about 180 mW. Of this, 50 mW is sent through an acousto-optic modulator (AOM) for the Zeeman slowing beam. The remaining 130 mW is used to produce

the three sets of MOT trapping beams. The frequency of the laser is manually adjusted to maximize the MOT fluorescence and then left untouched during the MOT loading time of 2 s. Since the drift of the Ti:sapphire laser is less than 10 MHz/h, the laser does not need to be actively locked. The optimal detuning for the MOT has been measured to be -30 MHz from resonance.

By contrast, the remaining three lasers need to be *locked* to their respective transitions. This is done in a separate spectroscopy chamber that has a collimated Yb atomic beam. The laser beams are sent perpendicular to the atoms, and the fluorescence is collected by two photomultiplier tubes (PMT, Hamamatsu R928). The scheme for locking the three lasers is shown in Fig. 3(a). The 556-nm beam is produced by doubling the output of a fiber laser operating at 1111 nm (Koheras Boostik Y10). The output power of the fiber laser is 0.5 W with a linewidth of 70 kHz. The total power in the 556-nm beam is 65 mW. For spectroscopy, a part of the beam is split into two and sent across the atomic beam in counterpropagating directions to minimize systematic Doppler shifts. A typical spectrum as the 556-nm laser is scanned across the ^{174}Yb peak is shown in Fig. 3(b). The laser is locked to the peak center by frequency modulation at 20 kHz and lock-in detection to generate the error signal.

The two lasers at 680 nm and 770 nm are home-built diode laser systems [21]. They are frequency stabilized using grating feedback to give linewidths of 1 MHz. The 680-nm beam counterpropagates with the locked 556-nm beam a few cm downstream from the 556-nm fluorescence point. As seen from the spectrum in Fig. 3(c), the 680-nm beam causes a decrease in the fluorescence as it pumps atoms into the metastable 3P_0 and 3P_2 states. The laser is again frequency modulated (at 15 kHz) and locked to the peak center. The 770-nm beam, which is a further 2 mm downstream and overlaps with the same 556-nm beam, causes the fluorescence to recover as it repumps atoms from the 3P_2 state back into the ground state. This increase is seen in the spectrum in Fig. 3(d). The 770-nm beam is modulated at a slightly different frequency from the

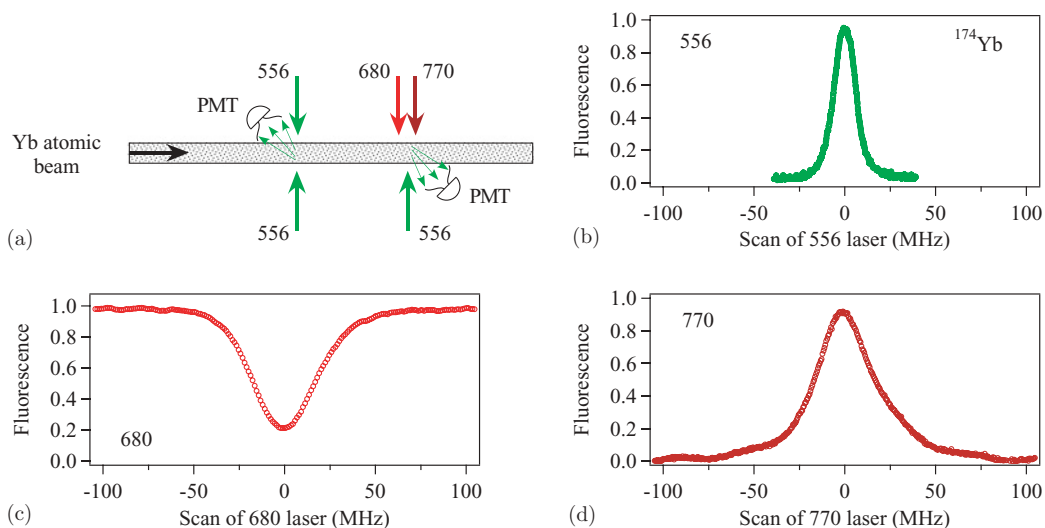


FIG. 3. (Color online) Schematic of the spectroscopy set-up for locking the 556, 680, and 770 lasers. The 770-nm beam is just a few mm downstream of the 680-nm beam (for state preparation), and both beams overlap with the counterpropagating 556-nm beam. Below are the fluorescence spectra for the three lasers.

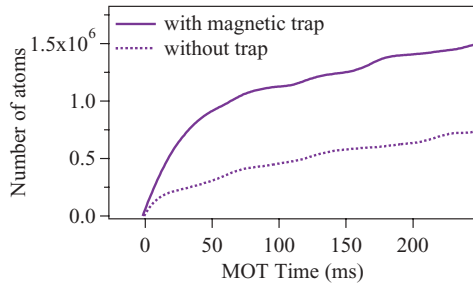


FIG. 4. (Color online) Change in the number of atoms in the MOT with and without the magnetic trap.

680-nm beam, and the same PMT signal is demodulated at this frequency to generate the error signal.

III. MAGNETIC TRAPPING RESULTS

The loading of the MOT proceeds as follows. The hot atoms emanating from the source are first slowed by the Zeeman slower. The slower beam is focused with a lens so that it has a size of 20 mm near the MOT and 4 mm at the differential pumping tube. The total power in the slowing beam is 20 mW. The six MOT beams are formed by taking three beams of the appropriate circular polarizations and retro-reflecting them. The beams have a power of 35 mW and size of 15 mm each. The axial field gradient for optimal operation of the MOT is 35 G/cm. The $^1S_0 \rightarrow ^1P_1$ transition used for the MOT is not closed since atoms can be lost to the metastable $^3P_{0,2}$ states through the intermediate D states (see Fig. 1). There are also losses due to background collisions in the vacuum chamber. These loss mechanisms limit the trap loading time constant to 1 s. We therefore load the trap for a total time of 2 s. This gives a cold cloud of size 3 mm. By calibrating the MOT fluorescence measured by the PMT, we estimate the number of atoms to be 10^7 . The temperature in the MOT is 3 ± 1 mK, measured by mapping the velocity distribution using time-of-flight 6 mm below the trap. This is a reasonable temperature in the MOT because the Doppler cooling limit of the 399-nm transition is 0.67 mK.

The cold atoms in the MOT are optically pumped from the ground state into the 3P_2 state by driving the $^1S_0 \rightarrow ^3P_1 \rightarrow ^3S_1$ transition with the 556-nm and 680-nm beams. From the 3S_1 state, atoms can decay into the $^3P_{0,1,2}$ states. Atoms which decay into the 3P_0 state are lost because the lifetime of this state is ~ 1 month, hence only a fraction goes into the desired 3P_2 state. These atoms are then magnetically trapped in a quadrupole trap using a field gradient of 110 G/cm. This field gradient produces a trap depth of 3.3 mK at a distance of 1.5 mm for $m_F = 2$ atoms, which is higher than the MOT temperature. During the magnetic trapping time, all laser beams are off. At the end of the trap period, the metastable atoms are pumped back to the ground state by the 770-nm beam, which drives the $^3P_2 \rightarrow ^3S_1$ transition. Again some fraction of atoms is lost to the 3P_0 state. The detection of the remaining atoms is done by turning on the MOT beams. The fluorescence as a function of time with and without the magnetic trap is shown in Fig. 4. Compared to the MOT without the magnetic trap, there is a jump in the initial

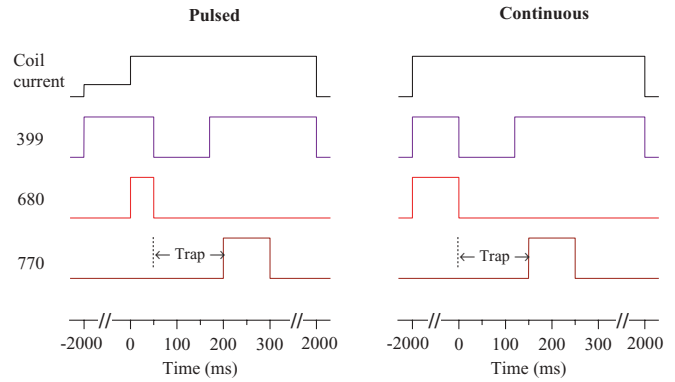


FIG. 5. (Color online) Sequence of magnetic-coil current and laser pulses for pulsed and continuous loading of the magnetic trap. The trap lasts from the time the 399-nm beam is turned off until the 770-nm beam is turned on.

fluorescence level since there is already a supply of cold atoms that can be recaptured.

We have studied both pulsed and continuous loading of the magnetic trap. The sequence of turning on the different laser beams for the two cases is shown in Fig. 5. Let us first look at the sequence for pulsed loading. Atoms are initially cooled and captured in the blue MOT for 2 s. At $t = 0$, the 680-nm beam is turned on. It has a size of 5 mm and power of 3 mW. The 556-nm beam is always on (not shown), therefore the 680-nm beam begins to pump atoms into the 3P_2 state. After 50 ms, both the 680-nm beam and the 399-nm (MOT) beams are turned off. The atoms are now magnetically trapped in the 3P_2 state. At the end of the magnetic-trapping period, the 770-nm beam is turned on. The beam has a power of 3 mW and a size of 5 mm. The MOT beams used for detecting the remaining atoms are turned on 30 ms before to prevent transients.

The main advantage of the pulsed loading scheme is that the current in the magnetic-field coils can be optimized separately for the MOT and the magnetic trap. Thus, it is initially kept at a low value (field gradient of 35 G/cm) during the MOT loading time and then ramped up to the magnetic-trap value (field gradient of 110 G/cm) at $t = 0$. By contrast, the continuous loading scheme requires the coil current to be high throughout, and hence the number of atoms captured in the MOT is not optimal. The other difference for this sequence, as seen from the figure, is that the 680-nm beam is on throughout the

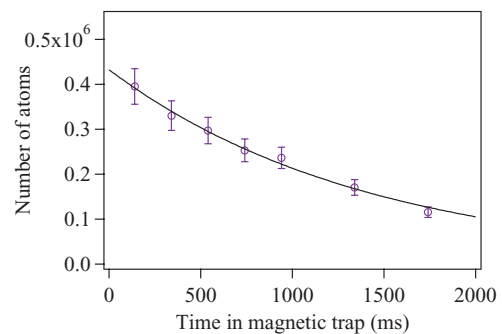


FIG. 6. (Color online) Lifetime of atoms in the magnetic trap. The solid line is a fit to an exponential decay, yielding a lifetime of 1.5 s.

MOT period so that atoms are continuously transferred into the 3P_2 state. This beam represents an additional loss rate from the MOT, hence its power is chosen to be sufficiently low ($<5 \mu\text{W}$) so that it does not prevent the MOT from forming. The size of the beam is about 1 mm and it is pointed at trap center, ensuring that only atoms from the low-velocity part of the distribution get pumped into the metastable state. At $t = 0$, all the laser beams are shut off and the magnetic trap is on. As before, the trapping ends when the 770-nm and MOT beams are turned on.

With the pulsed loading scheme and the use of an optimized field gradient, we are able to capture up to 10^7 atoms in the MOT in 2 s. Of these, roughly 10% get pumped into the 3P_2 state and are magnetically trapped. In the continuous loading case, the number of atoms in the MOT is only 2×10^6 . In both cases, we have studied the lifetime by studying the number of atoms surviving as a function of trap time. The results for pulsed loading of the trap are shown in Fig. 6. In this particular run, the trap had about 0.5 million atoms in the beginning. The solid line is a fit to an exponential decay, yielding a lifetime of 1.5 s. This lifetime is reasonable given the vacuum level in our chamber and that the atomic beam is always on, leading to losses due to collisions with background atoms and with hot Yb atoms. This is also consistent with the slightly smaller MOT time constant of 1 s, which has additional losses due to decay into the metastable states.

IV. CONCLUSIONS

In conclusion, we have demonstrated trapping of Yb atoms in the spectroscopically important 3P_2 excited (metastable) state. Atoms are first cooled and trapped in the ground state in a MOT operating on the $^1S_0 \rightarrow ^1P_1$ line. They are then

transferred to the excited state via the upper 3S_1 state. The trap is a spherical quadrupole trap with an axial field gradient of 110 G/cm. The trapped atoms are detected by turning the MOT back on and looking at the initial fluorescence. We load up to 10^7 atoms in the MOT from a Zeeman-slowed atomic beam, and then transfer 10% into the magnetic trap. Atoms in the trap have a lifetime of 1.5 s.

In this experiment, we did not strive to achieve the best vacuum or incorporate a beam shutter to turn off the atomic beam during the magnetic trap period. With these improvements, the background-limited lifetime can be improved by at least an order of magnitude. In particular, the number of atoms in the MOT, which is a competition between the loading rate and the loss rate (due to background collisions), will increase significantly. This will increase the number of atoms transferred to the metastable state in both the pulsed and continuous loading schemes. Moreover, the state preparation in the 3P_2 state and detection by repumping into the ground state are limited by losses due to decay into the 3P_0 state. Atoms going into this state can be recovered by using a laser at 649 nm to drive the $^3P_0 \rightarrow ^3S_1$ transition. With this additional laser, all the atoms in the MOT can be pumped into the 3P_2 state. We are in the process of incorporating this laser into our experiment.

ACKNOWLEDGMENTS

We thank V. Anandan of the glass-blowing section for fabricating the multiport pyrex chamber. This work was supported by the Department of Science and Technology. K.P. acknowledges financial support from the Council of Scientific and Industrial Research and S.B.P. from the Kishore Vaigyanik Protsahan Yojana, Government of India.

-
- [1] A. P. Mishra and T. K. Balasubramanian, *J. Quant. Spectrosc. Radiat. Transfer* **69**, 769 (2001).
 - [2] Z. W. Barber, C. W. Hoyt, C. W. Oates, L. Hollberg, A. V. Taichenachev, and V. I. Yudin, *Phys. Rev. Lett.* **96**, 083002 (2006).
 - [3] A. Derevianko and C. C. Cannon, *Phys. Rev. A* **70**, 062319 (2004).
 - [4] K. Shibata, S. Kato, A. Yamaguchi, S. Uetake, and Y. Takahashi, *Appl. Phys. B* **97**, 753 (2009).
 - [5] V. Natarajan, *Eur. Phys. J. D* **32**, 33 (2005).
 - [6] P. G. H. Sandars, *Phys. Lett.* **22**, 290 (1966).
 - [7] D. Hansen and A. Hemmerich, *Phys. Rev. Lett.* **96**, 073003 (2006).
 - [8] A. Traverso, R. Chakraborty, Y. N. M. de Escobar, P. G. Mickelson, S. B. Nagel, M. Yan, and T. C. Killian, *Phys. Rev. A* **79**, 060702(R) (2009).
 - [9] Y. Takasu, K. Maki, K. Komori, T. Takano, K. Honda, M. Kumakura, T. Yabuzaki, and Y. Takahashi, *Phys. Rev. Lett.* **91**, 040404 (2003).
 - [10] T. Fukuhara, S. Sugawa, and Y. Takahashi, *Phys. Rev. A* **76**, 051604(R) (2007).
 - [11] S. Stellmer, M. K. Tey, B. Huang, R. Grimm, and F. Schreck, *Phys. Rev. Lett.* **103**, 200401 (2009).
 - [12] Y. N. Martinez de Escobar, P. G. Mickelson, M. Yan, B. J. DeSalvo, S. B. Nagel, and T. C. Killian, *Phys. Rev. Lett.* **103**, 200402 (2009).
 - [13] A. Yamaguchi, S. Uetake, D. Hashimoto, J. M. Doyle, and Y. Takahashi, *Phys. Rev. Lett.* **101**, 233002 (2008).
 - [14] A. Griesmaier, J. Werner, S. Hensler, J. Stuhler, and T. Pfau, *Phys. Rev. Lett.* **94**, 160401 (2005).
 - [15] U. D. Rapol, A. Krishna, A. Wasan, and V. Natarajan, *Eur. Phys. J. D* **29**, 409 (2004).
 - [16] K. Honda, Y. Takahashi, T. Kuwamoto, M. Fujimoto, K. Toyoda, K. Ishikawa, and T. Yabuzaki, *Phys. Rev. A* **59**, R934 (1999).
 - [17] T. Loftus, J. R. Bochinski, R. Shivitz, and T. W. Mossberg, *Phys. Rev. A* **61**, 051401(R) (2000).
 - [18] T. Kuwamoto, K. Honda, Y. Takahashi, and T. Yabuzaki, *Phys. Rev. A* **60**, R745 (1999).
 - [19] S. B. Nagel, C. E. Simien, S. Laha, P. Gupta, V. S. Ashoka, and T. C. Killian, *Phys. Rev. A* **67**, 011401(R) (2003).
 - [20] A. Chikkatur, Ph.D. thesis, Massachusetts Institute of Technology, Cambridge (2002).
 - [21] A. Banerjee, U. D. Rapol, A. Wasan, and V. Natarajan, *Appl. Phys. Lett.* **79**, 2139 (2001).